Chinese Physical Society | IOP Publishing
CPB
Chinese Physics B
http://cpb.iphy.ac.cn https://iopscience.iop.org/journal/1674-1056

Magnetoelastic coupling effect of $Fe_{10}Co_{90}$ films grown on different flexible substrates

Jiapeng Zhao(赵佳鹏), Qinhuang Guo(郭勤皇), Huizhong Yin(尹慧中), Jintang Zou(邹锦堂), Zhenjie Zhao(赵振杰), Wenjuan Cheng(程文娟), Dongmei Jiang(蒋冬梅), Qingfeng Zhan(詹清峰)

Citation: Chin. Phys. B . 2020, 29(11): 117501 . **doi:** 10.1088/1674-1056/abb22d
Journal homepage: http://cpb.iphy.ac.cn; http://iopscience.iop.org/cpb

What follows is a list of articles you may be interested in

Giant anisotropy of magnetic damping and significant in-plane uniaxial magnetic anisotropy in amorphous $Co_{40}Fe_{40}B_{20}$ films on GaAs(001)

Ji Wang(王佶), Hong-Qing Tu(涂宏庆), Jian Liang(梁健), Ya Zhai(翟亚), Ruo-Bai Liu(刘若柏), Yuan Yuan(袁源), Lin-Ao Huang(黄林傲), Tian-Yu Liu(刘天宇), Bo Liu(刘波), Hao Meng(孟皓), Biao You(游彪), Wei Zhang(张维), Yong-Bing Xu(徐永兵), Jun Du(杜军)

Chin. Phys. B . 2020, 29(10): 107503 . **doi:** 10.1088/1674-1056/abad1d

Thickness-dependent magnetic anisotropy in obliquely deposited Fe(001)/Pd thin film bilayers probed by VNA-FMR

Qeemat Gul, Wei He(何为), Yan Li(李岩), Rui Sun(孙瑞), Na Li(李娜), Xu Yang(杨旭), Yang Li(李阳), Zi-Zhao Gong(弓子召), Zong-Kai Xie(谢宗凯), Xiang-Qun Zhang(张向群), Zhao-Hua Cheng(成昭华)

Chin. Phys. B . 2019, 28(7): 077502 . **doi:** 10.1088/1674-1056/28/7/077502

Thickness dependent manipulation of uniaxial magnetic anisotropy in Fe-thin films by oblique deposition

Qeemat Gul, Wei He(何为), Yan Li(李岩), Rui Sun(孙瑞), Na Li(李娜), Xu Yang(杨旭), Yang Li(李阳), Zi-Zhao Gong(弓子召), ZongKai Xie(谢宗凯), Xiang-Qun Zhang(张向群), Zhao-Hua Cheng(成昭华)

Chin. Phys. B . 2018, 27(9): 097504 . **doi:** 10.1088/1674-1056/27/9/097504

Diverse features of magnetization curves of uniaxial crystals: A simulation study

Hala A. Sobh, Samy H. Aly

Chin. Phys. B . 2017, 26(1): 017503 . **doi:** 10.1088/1674-1056/26/1/017503

Manipulating magnetic anisotropies of Co/MgO(001) ultrathin films via oblique deposition

Syed Sheraz Ahmad, Wei He(何为), Jin Tang(汤进), Yong Sheng Zhang(张永圣), Bo Hu(胡泊), Jun Ye(叶军), Qeemat Gul, Xiang-Qun Zhang(张向群), Zhao-Hua Cheng(成昭华)

Chin. Phys. B . 2016, 25(9): 097501 . **doi:** 10.1088/1674-1056/25/9/097501

Chin. Phys. B Vol. 29, No. 11 (2020) 117501

Magnetoelastic coupling effect of $Fe_{10}Co_{90}$ films grown on different flexible substrates*

Jiapeng Zhao(赵佳鹏)[1], Qinhuang Guo(郭勤皇)[1], Huizhong Yin(尹慧中)[1], Jintang Zou(邹锦堂)[2], Zhenjie Zhao(赵振杰)[2], Wenjuan Cheng(程文娟)[2,†], Dongmei Jiang(蒋冬梅)[1], and Qingfeng Zhan(詹清峰)[1,‡]

[1] *Key Laboratory of Polar Materials and Devices (MOE) and State Key Laboratory of Precision Spectroscopy, School of Physics and Electronic Science, East China Normal University, Shanghai* 200241, *China*

[2] *Engineering Research Center for Nanophotonics and Advanced Instrument, School of Physics and Electronic Science, East China Normal University, Ministry of Education, Shanghai* 200241, *China*

(Received 10 May 2020; revised manuscript received 22 July 2020; accepted manuscript online 25 August 2020)

The magneto–mechanical coupling effect and magnetic anisotropy of $Fe_{10}Co_{90}$ (FeCo) films deposited on silicon wafer (Si), flexible polyethylene terephthalate (PET), freestanding polydimethylsiloxane (PDMS), and pre-stretched 20% PDMS substrates were studied in detail. The loop squareness ratio M_r/M_s and the coercive H_c of the FeCo film grown on a PET substrate can be obviously tuned by applying a small tensile-bending strain, and those of the FeCo film grown on a freestanding PDMS substrate can only be slightly changed when applying a relatively large tensile bending strain. For the FeCo film prepared on a 20% pre-stretched PDMS, a wrinkled morphology is obtained after removing the pre-strain. The wrinkled FeCo film can keep the magnetic properties unchanged when applying a relatively large tensile bending strain perpendicular to the wrinkles. This reveals that PDMS is an ideal substrate for magnetic films to realize flexible immutability. Our results may help for developing flexible magnetic devices.

Keywords: flexible substrates, FeCo films, magnetic anisotropy, magneto–mechanical coupling effect

PACS: 75.40.Cx, 75.70.Ak, 75.30.Gw, 75.75.Cd **DOI:** 10.1088/1674-1056/abb22d

1. Introduction

Magnetic thin films possess essentially different magnetic properties compared with bulk counterparts, and have been rapidly exploited for information processing and storage application as magnetoelectronic components, especially the magnetic anisotropy of magnetic thin films has attracted much attention. For instance, the magnetic anisotropy of magnetic thin films applied in microwave devices is one of the most critical decisive factors for ferromagnetic resonance frequency on the basis of the Kittel equation.[1,2] And in magnetic sensors, the magnetic field sensitivity is determined by the magnetic anisotropy of the magnetic sensing layer.[3] Obviously, it is extremely vital to manipulate the magnetic anisotropy in magnetic films. Normally, there are some technical methods to effectively tune the magnetic anisotropy of magnetic films, such as oblique deposition,[4–6] annealing under magnetic field,[7] and exchange bias.[8] Recently, the magnetic anisotropy could be changed by modifying the surface topography of magnetic thin films.[9–13] For example, Chen *et al.* employed ion beam etching to produce a rippled structure on the surface of Co films, resulting in a significant uniaxial magnetic anisotropy.[14] Ki *et al.* used a thermal annealing method to obtain a triangular wrinkled morphology on m-plane Al_2O_3 substrate, and the NiFe thin films grown on the wave-like surface exhibited a rather strong magnetic anisotropy.[15]

Since flexible electronic devices have been widely used in wearable intelligent devices and related fields, the deposition of magnetic films on flexible substrates to obtain flexible electronic devices becomes one of the most critical research fields, which opens up new potential applications of flexible display screens,[16] flexible microwave absorbing devices,[17] and flexible magnetic memory.[3] Flexible substrates possess various advantages, such as wear resistance, high bending degree, low-cost, etc., which play a key role in many applications. Previous investigation revealed that substrate deformations can transfer bending strains to magnetic layers when they are deposited onto flexible membranes. Thus, it is extremely vital to investigate how magnetic properties of electronic devices are adjusted with the deformation of flexible substrates.[18] The magnetic anisotropy of magnetic films sputtered on different flexible substrates including polyimide (PI),[19] polyethylene terephthalate (PET),[20] and mica[21,22] can be tuned by applying tensile bending strains, thereby affecting the performance of the electronic device. Although this is a significant property for tunable magnetic anisotropy applications, it is still desirable for maintaining inherent magnetic properties to take effective measures. Recently, $Fe_{10}Co_{90}$ (FeCo) alloy, showing a sizable magnetostriction ($\lambda_s \sim 60 \times 10^{-6}$ for the typical bulk), possessing a high spin polarization, and having a large magnetic resistance ratio, has been usually cho-

*Project supported by the National Natural Science Foundation of China (Grant Nos. 11674336 and 11874150).

†Corresponding author. E-mail: wjcheng@phy.ecnu.edu.cn

‡Corresponding author. E-mail: qfzhan@phy.ecnu.edu.cn

sen as the magnetic free layer in numerous applications of spintronic devices.[23] So far, there is no systematical research on the magneto-mechanical coupling effect and uniaxial magnetic anisotropy of FeCo films deposited on different flexible membranes. Here, the uniaxial magnetic anisotropy of FeCo films deposited on Si, PET, and PDMS substrates were systematically investigated. Compared with the FeCo film on Si, FeCo films on PET and PDMS membranes have the vast advantage in maintaining lossless properties under a small tensile bending strain. The uniaxial magnetic anisotropy of the FeCo film on the PET substrate can be effectively tuned by applying a small tensile bending strain, while the magnetic properties of the FeCo film on the freestanding PDMS substrate have a slight change by applying a relatively large tensile bending strain. In contrast, the magnetic properties of the wrinkled FeCo film on the pre-stretched PDMS membrane remain nearly constant with applying a relatively large tensile bending strain perpendicular to the wrinkles. These findings are important for the development of flexible electronic devices.

2. Experiment

Using a radio frequency magnetron sputtering system with a base pressure lower than 5.0×10^{-4} Pa, FeCo films with a thickness of 40 nm were deposited on Si, PET, freestanding PDMS, and 20% pre-stretched PDMS substrates, respectively. Before introducing the substrates into the sputtering chamber, they were cleaned ultrasonically in alcohol, and then dried with argon gas. During deposition, the argon flow was maintained at 25.5 sccm and the pressure was adjusted to 2.1 Pa. The deposition rate of the FeCo films was 4 nm/min. In order to prevent FeCo atoms from entering the flexible polymer substrate, a buffer layer of 6 nm Ta was firstly deposited on the substrates. Prior to be taken out of the chamber, a 6 nm Ta capping layer was deposited on the FeCo films to avoid oxidation. The surface topography was measured by utilizing atomic force microscopy (AFM) in a non-contact scanning mode. The magnetic hysteresis loops were collected by using vibrating sample magnetometer (VSM, Lake Shore 7410). In order to determine the coercivity with high precision, a step of 2.5 Oe was used to sweep the magnetic field close to the coercive field of the FeCo films. All the characterizations were performed at room temperature.

3. Result and discussion

Figures 1(a)–1(c) exhibit the three-dimensional (3D) topography of bare Si, PET, and freestanding PDMS substrates, while figures 1(d)–1(f) show the 3D morphology of Ta/FeCo/Ta thin films prepared on the different substrates. The Si, PET, and PDMS substrates possess pretty diverse root-mean-square (RMS) roughnesses around 0.63 nm, 2.79 nm, and 2.78 nm, respectively. After depositing metallic films, the RMS roughnesses of Ta/FeCo/Ta on Si, PET, and PDMS substrates become 1.08 nm, 3.50 nm, and 5.87 nm, respectively. It can be seen that the influence of the substrate roughness on the metallic films is extremely dominant. A closer examination of Figs. 1(d)–1(f) evidently indicates an obvious “sags and crests” character for the films on the PET and PDMS substrates but not for the film on the Si substrate, where the metallic surface reveals a mass of deep ridges not uniformly leveled. Therefore, the RMS roughness for the sample grown on the freestanding PDMS membrane is the largest, while it is the smallest for the film on the Si substrate.

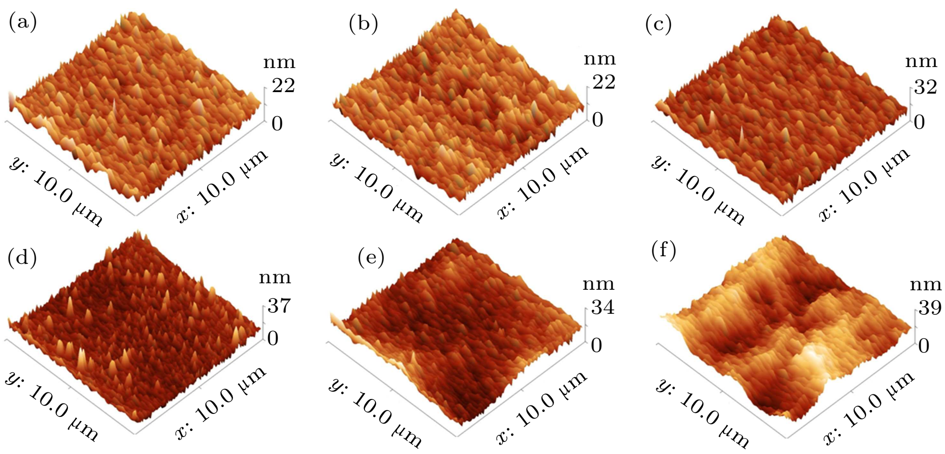

Fig. 1. AFM images (10×10 μm^2) of bare substrates of (a) rigid Si, (b) flexible PET, and (c) soft PDMS. AFM images (10×10 μm^2) of the stacks of Ta(6 nm)/FeCo(40 nm)/Ta(6 nm) deposited on (d) Si, (e) PET, and (f) PDMS substrates.

In order to check the in-plane magnetic anisotropy of the FeCo films deposited on different substrates, the magnetic hysteresis loops were measured at different field orientations θ. As depicted in Figs. 2(a) and 2(b), the loop squareness ratio M_r/M_s and the coercivity H_c of all samples oscillate with a periodicity of 180°, showing a uniaxial magnetic anisotropy. Figures 2(c)–2(e) exhibit the typical hysteresis loops along the easy and hard axes of the FeCo films deposited on Si, PET, and PDMS substrates. For the measurements along the easy axis, the coercivities of the FeCo films on Si, PET, and PDMS substrates are 33 Oe, 38 Oe, and 40 Oe, respectively, while the corresponding loop squareness ratios are 0.99, 0.97, and 0.83. For the measurements along the hard axis, the corresponding coercivities are 24 Oe, 13 Oe, and 31 Oe, while the loop squareness ratios are 0.24, 0.13, and 0.55. For the measurement along the easy axis, H_c for the FeCo film grown on the freestanding PDMS nearly equals, within the measurement error, to that of the FeCo film on the PET substrate, both of them are greater than H_c of the FeCo film on Si. This indicates that the RMS roughness of different substrates can remarkably influence the coercive field of the FeCo films. The uniaxial magnetic anisotropy K_u of FeCo films can be estimated from the difference of the area enclosed between the hysteresis loops measured along the easy and hard axes.[24,25] The obtained K_u of the FeCo films on the Si, PET, and freestanding PDMS substrates are 1.11×10^3 erg/cm^3, 1.54×10^3 erg/cm^3, and 3.71×10^2 erg/cm^3, respectively. The uniaxial magnetic anisotropy can be understood by considering the residual stress of the FeCo films grown on different substrates. The inevitable micro-deformation of flexible PET and PDMS substrates during the deposition process may transfer to the FeCo films, inducing a uniaxial magnetic anisotropy due to the magnetostriction effect.[26] However, the residual stress can be effectively relaxed for the FeCo film grown on the freestanding PDMS membrane due to the extremely small elastic coefficient of PDMS. Thus, the FeCo film on the freestanding PDMS membrane displays the smallest uniaxial magnetic anisotropy. In addition, the FeCo film deposited on the rigid Si substrate exhibits a significant uniaxial magnetic anisotropy, which originates from both the residual stress and the atomic steps existing on the surface of the Si substrate.

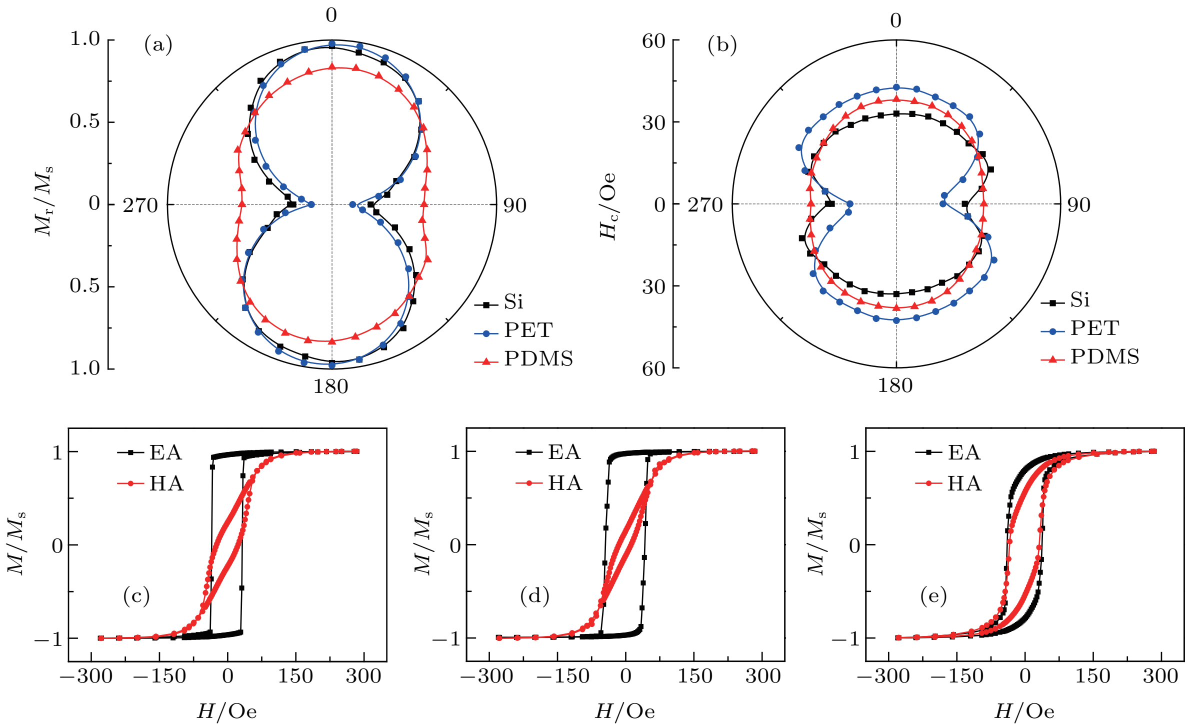

Fig. 2. Angular dependence of (a) the loop squareness ratio M_r/M_s and (b) the coercivity H_c for the FeCo films grown on Si, PET, and freestanding PDMS substrates. The hysteresis loops measured along the easy axis (EA) and the hard axis (HA) for the FeCo films grown on Si, PET, and freestanding PDMS substrates.

Although both PET and PDMS are flexible substrates, due to their different elastic moduli which can induce various strains onto metal films deposited on them, they have a disparate impact on the magnetic properties of FeCo films. In order to study the strain dependent magnetic anisotropy for the FeCo films grown on PET and PDMS membranes, several semi-cylindrical molds with various radii of curvature were designed by using teflon materials. The samples were fixed onto the convex surface of the molds to obtain different tensile bending strains. The strain s can be evaluated by using the relation $s = d/2\rho$, where d is the total thickness of both the substrate and the film, and ρ is the curvature radius of the convex surface of the molds. Using the convex molds, the strains in the FeCo film on the PET substrate can be varied from 0 to 1.2% with an increment of 0.4%. For the magnetic measurements, the strain was applied by tensile bending the sample along the easy or hard axis, and the in-plane magnetic field was applied perpendicular to the tensile bending direction. Thus, the magnetic field can be restricted parallel to the film plane. Figures 3(a) and 3(b) exhibit the hysteresis loops measured along the easy and hard axes of the FeCo film on the PET substrate under various tensile bending strains along the hard and easy axes, respectively. By applying the magnetic field along the easy axis and increasing the tensile bending strain along the hard axis from 0 to 1.2%, H_c increases from 38 Oe to 50 Oe, and the M_r/M_s ratio slightly goes up from 0.97 to 0.98, as shown in the inset of Fig. 3(a). When the magnetic field is applied along the hard axis of the FeCo film, the increase of tensile bending strain along the easy axis from 0 to 1.2% leads to increases of H_c from 13 Oe to 22 Oe and of the M_r/M_s ratio from 0.13 to 0.31, as shown in the inset of Fig. 3(b). Obviously, the magnetic properties of the FeCo films strongly depend on the applied tensile bending strain through the magneto-mechanical coupling effect.[26,27]

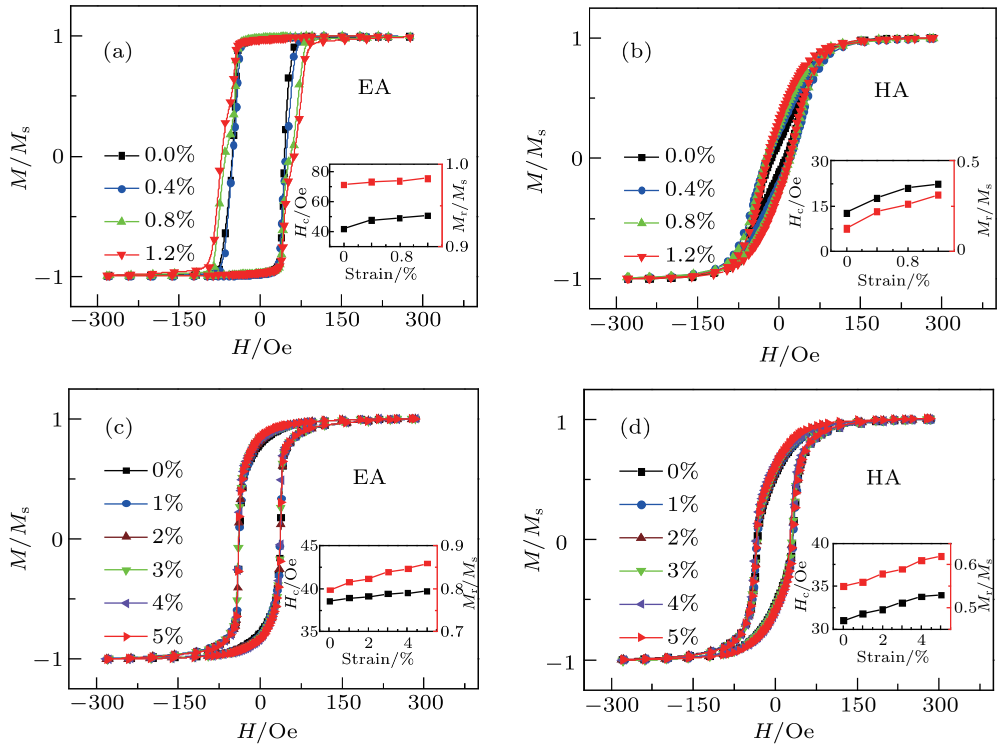

Fig. 3. Hysteresis loops for FeCo films grown on the PET substrate acquired with magnetic field applied along (a) the easy axis (EA) and (b) the hard axis (HA) with different external tensile bending strains applied along the hard axis and the easy axis, respectively. Hysteresis loops for FeCo films grown on the freestanding PDMS substrate acquired with magnetic field applied along (c) the easy axis and (d) the hard axis with different external tensile bending strains applied along the hard axis and the easy axis, respectively. The insets correspondingly show the tensile bending strain dependence of the M_r/M_s ratio and the coercivity.

Because the elastic coefficient of PDMS substrate is much smaller than that of PET substrate. Compared with the PET substrate, the PDMS substrate can be easily bent. Figures 3(c) and 3(d) display the hysteresis loops measured with the magnetic field applied along the easy and hard axes for the FeCo film grown on the freestanding PDMS substrate under various tensile bending strains applied along the hard and easy axes, respectively. The tensile bending strain increases from 0 to 5% with an increment of 1% by using the above-mentioned semi-cylindrical molds. For the tensile bending strain applied along the hard axis, H_c measured along the easy axis slightly increases from 38 Oe to 40 Oe and the M_r/M_s ratio increases from 0.76 to 0.83. For the tensile bending strain applied along the easy axis, H_c along the hard axis slightly increases from 31 Oe to 34 Oe and the M_r/M_s ratio increases from 0.55 to 0.62, as shown in the insets of Figs. 3(c) and 3(d). Thus, the magnetic properties of the FeCo film grown on the freestanding PDMS substrate can slightly be regulated with applying external tensile bending strains.

Compared with the FeCo film prepared on the freestanding PDMS substrate, the FeCo film deposited on a prestrained PDMS substrate exhibits an anisotropic wrinkled surface structure. The wrinkled morphology may significantly change the magnetic properties of the films. The identical stacks of Ta(6 nm)/FeCo(40 nm)/Ta(6 nm) film were sputtered on a 20% pre-strained PDMS substrate by using a home-made stretching apparatus. After the pre-strain of 20% was removed from the sample, an ordered wavy wrinkled structure with a wavelength of 7.56 μm and an amplitude of 1.30 μm appeared on the surface, as shown in Fig. 4(a). The formation of such a wrinkled surface originates from the mismatch of elastic moduli between the rigid metal layer and the elastomeric PDMS substrate. The wavelength λ and the amplitude h of the buckling pattern can be described as

$$\lambda \approx \frac{\pi t}{\sqrt{\varepsilon_c}},$$

$$h = t\left(\frac{\varepsilon_{\mathrm{PDMS}}}{\varepsilon_c} - 1\right)^{1/2},$$

$$\varepsilon_{\mathrm{c}} = 0.52\left[\frac{E_{\mathrm{PDMS}}\left(1-\upsilon_M^2\right)}{E_M\left(1-\upsilon_{\mathrm{PDMS}}^2\right)}\right]^{2/3},$$

where ε_{c} is a physical quantity representing the certain threshold strain for wrinkle, $\varepsilon_{\mathrm{PDMS}}$ is the pre-strain applied on PDMS, and t is the metallic layer thickness. E and v are the Young's modulus and the Poisson ratio, respectively. The subscriptions M and PDMS mean the metallic layer and the flexible substrate, respectively.[28–30] It is obvious that the wavelength of buckling is not only determined by the total thicknesses of the metallic layers but also influenced by the film/substrate modulus ratio. Based on the formerly reported elastic parameters for bulk alloys ($E_{\mathrm{Ta}} = 100$ GPa, $E_{\mathrm{FeCo}} = 200$ GPa, and $\upsilon_M = 0.31$) and PDMS membranes ($E_{\mathrm{PDMS}} = 1$ MPa and $\upsilon_{\mathrm{PDMS}} = 0.5$),[31–33] the wavelength λ and the amplitude h predicted by the theoretical equations are 7.76 μm and 1.10 μm, respectively. Considering the difference between the Young's moduli of metal film and bulk counterpart, the predicted values agree well with our experimental results. The magnetic hysteresis loops were measured at different field orientations θ with respect to the wrinkles, so as to investigate the in-plane magnetic anisotropy of the wrinkled FeCo film. As shown in Fig. 4(c), the angular dependences of the $M_{\mathrm{r}}/M_{\mathrm{s}}$ ratio and H_{c} oscillate with a periodicity of 180°. They both show the maximum and minimum values at $\theta = 0°$ and $\theta = 90°$, respectively, demonstrating a uniaxial magnetic anisotropy with the easy axis along the wrinkles and the hard axis perpendicular to the wrinkles. Figure 4(c) exhibits the typical magnetic hysteresis loops with the magnetic field applied parallel and perpendicular to the wrinkles of the film. The $M_{\mathrm{r}}/M_{\mathrm{s}}$ ratio and H_{c} acquired along the easy axis show the maximum values of 0.80 and 48 Oe, respectively. In contrast, the $M_{\mathrm{r}}/M_{\mathrm{s}}$ ratio and H_{c} exhibit the minimum values of 0.57 and 36 Oe along the hard axis, respectively. The uniaxial magnetic anisotropy K_{u} of the wrinkled FeCo film is estimated to be 4.64×10^2 erg/cm^3,[24,25] which is stronger than that of the FeCo film grown on the freestanding PDMS. The wrinkled surface structure can be viewed as an anisotropic surface roughness, which therefore gives rise to an enhanced K_{u}. When a saturation magnetic field applied perpendicular to the wrinkles aligns the FeCo magnetization parallel to the film plane, magnetic charges are accumulated on the wrinkled surface. The dipolar interaction between the magnetic charges serves as a coupling field favoring parallel alignment of the magnetization, which could induce a surface anisotropy with the easy axis along the wrinkles.

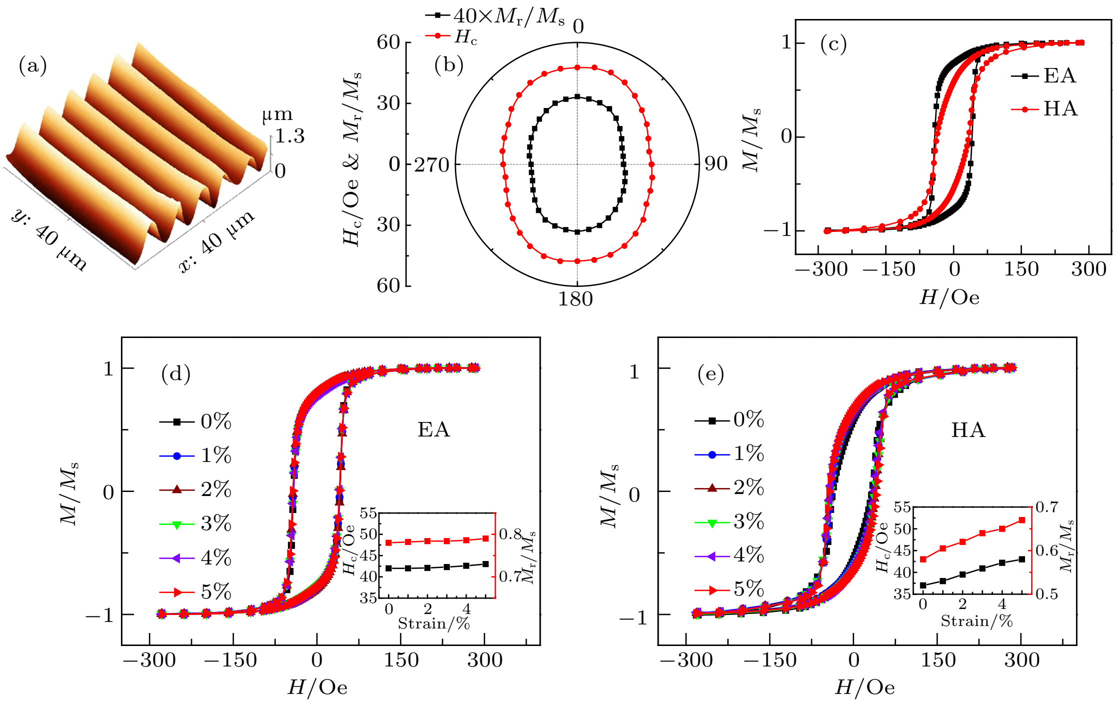

Fig. 4. (a) AFM image (40×40 μm^2) for the wrinkled FeCo film grown on a 20% pre-stretched PDMS. (b) The corresponding angular dependence of the loop squareness ratio $M_{\mathrm{r}}/M_{\mathrm{s}}$ and the coercive field H_{c}. (c) The typical hysteresis loops for the wrinkled FeCo film measured along the easy and hard axes. Hysteresis loops for the wrinkled FeCo film acquired along (d) the easy axis and (e) the hard axis with different external tensile bending strains applied perpendicular and parallel to the wrinkles, respectively. The insets correspondingly show the tensile bending strain dependence of the $M_{\mathrm{r}}/M_{\mathrm{s}}$ ratio and the coercivity.

In order to investigate the magneto–mechanical coupling effect in the FeCo film with buckling, the hysteresis loops were measured along the easy and hard axes with the tensile bending strains applied perpendicular to the magnetic field, i.e., along the hard and easy axes, respectively, as shown in Figs. 4(d) and 4(e). The strains were varied from 0 to 5% with an increment of 1%. The strain dependence of the $M_{\mathrm{r}}/M_{\mathrm{s}}$ ratio and H_{c} are summarized in the insets of Figs. 4(d) and

4(e). By increasing the tensile bending strain applied along the hard axis from 0 to 5%, H_c obtained along the easy axis increases from 44 Oe to 48 Oe and the M_r/M_s ratio increases from 0.79 to 0.81. When increasing the tensile bending strain applied along the easy axis from 0 to 5%, H_c obtained along the hard axis increases from 37 Oe to 43 Oe and the M_r/M_s ratio increases from 0.58 to 0.66. Obviously, the tensile bending strain applied perpendicular to the wrinkles has less influence on the magnetic properties of the wrinkled FeCo film measured with the magnetic field applied parallel to the wrinkles, which is because the large tensile bending strain can be relaxed through the wavelike wrinkled surface structure.[34,35]

4. Conclusion

In summary, FeCo films of 40 nm in thickness were deposited on Si, PET, freestanding PDMS, and 20%pre-stretched PDMS substrates by magnetron sputtering. Due to the magneto–mechanical coupling effect, the M_r/M_s ratio and H_c increase with the tensile bending strain increasing from 0 to 1.2% along the easy or hard axis for the FeCo film grown on the PET substrate. In contrast, for the FeCo film deposited on the freestanding PDMS substrate, the M_r/M_s ratio and H_c display only a slightly change with the tensile bending strain increasing from 0 to 5%, which indicates that the magnetoelastic coupling between the metal film and the PDMS substrate is extremely weak. For the wrinkled FeCo film grown on a pre-stretched PDMS, with the tensile bending strain increasing from 0 to 5%, both the M_r/M_s ratio and H_c measured along the wrinkled structure almost remain stable, and the M_r/M_s ratio and H_c measured perpendicular to the hard axis show a slightly change. It reveals that the wrinkled morphology can improve the stability of the magnetic properties. Therefore, PDMS membranes, as flexible substrates, are a good candidate for fabricating flexible electronic devices and realizing the flexibility.

References

[1] Kittel C 1947 *Phys. Rev.* **71** 270
[2] Phuoc N N, Chapon P, Acher O and Ong C K 2013 *J. Appl. Phys.* **114** 153903
[3] Quandt E and Ludwig A 1999 *J. Appl. Phys.* **85** 6232
[4] Lisfi A, Lodder J C, Wormeester H and Poelsema B 2002 *Phys. Rev. B* **66** 174420
[5] Fan X, Xue D, Lin M, Zhang Z, Guo D, Jiang C and Wei J 2008 *Appl. Phys. Lett.* **92** 222505
[6] Qeemat Gul, He W, Li Y, Sun R, Li N, Yang X, Li Y, Gong Z Z, Xie Z K, Zhang X Q and Cheng Z H 2018 *Chin. Phys. B* **27** 097504
[7] Yoo J H, Restorff J B, Wun-Fogle M and Flatau A B 2008 *J. Appl. Phys.* **103** 07B325
[8] Kuanr B K, Camley R E and Celinski Z 2003 *J. Appl. Phys.* **93** 7723
[9] Thevenard L, Zeng H T, Petit D and Cowburn R P 2009 *Appl. Phys. Lett.* **95** 232502
[10] Ziberi B, Frost F, Höoche T and Rauschenbach B 2005 *Phys. Rev. B* **72** 235310
[11] Vaz C A F, Steinmuller S J and Bland J A C 2007 *Phys. Rev. B* **75** 132402
[12] Liedke M O, Körner M, Lenz K, Fritzsche M, Ranjan M, Keller A and Lindner J 2013 *Phys. Rev. B* **87** 024424
[13] Liu H L, Volodin A, Temst K, Vantomme A and C Van Haesendonck 2015 *Phys. Rev. B* **91** 104403
[14] Chen K, Frömter R, Rössler S, Mikuszeit N and Oepen H P 2012 *Phys. Rev. B* **86** 064432
[15] Ki S and Dho J 2015 *Appl. Phys. Lett.* **106** 212404
[16] Yang Y, Yuan G, Yan Z, Wang Y, Lu X and Liu J M 2017 *Adv. Mater.*
[17] Wang X W, Gu Y, Xiong Z P, Cui Z and Zhang T 2014 *Adv. Mater* **26** 1336
[18] Nishibe Y, Yamadera H, Ohta N, Tsukada K and Ohmura Y 2003 *IEEE. Trans. Magn.* **39** 571
[19] Zhang H, Li Y Y, Yang M Y, Zhang B, Yang G, Wang S G and Wang K Y 2015 *Chin. Phys. B* **24** 077501
[20] Guohong Dai, Xiangjun Xing, Yun Shen and Xiaohua Deng 2020 *J. Phys. D: Appl. Phys.* **53** 055001
[21] Yang Y X, Yuan G L, Yan Z B, Wang Y J, Lu X B and Liu J M 2017 *Adv. Mater.*
[22] Xiaohui Shi, Mei Wu, Zhengxun Lai, Xujing Li, Peng Gao and Wenbo Mi 2020 *ACS Appl. Mater. Interfaces* **12** 27394
[23] Zhou L 2014 *Research and exploration of new Fe-based magnetostrictive materials*, (Master Dissertation) (HeBei: HeBei University of Technology) (in Chinese)
[24] Johnson M T, Bloemen P H, F J A den Broeder and J de Vries 1996 *Rep. Prog. Phys.* **59** 1409
[25] Zhang X S, Zhan Q F, Dai G H, Liu Y W, Zuo Z H, Yang H L, Chen B and Li R W 2013 *Appl. Phys. Lett.* **113** 17A901
[26] Dai G H, Zhan Q F, Liu Y W, Yang H L, Zhang X S, Chen B and Li R W 2012 *Appl. Phys. Lett.* **114** 173913
[27] Khang D Y, Jiang H J, Huang Y and Rogers J A 2006 *Science* **311** 208
[28] Chen X and Hutchinson J W 2004 *J. Appl. Mech.* **71** 597
[29] Huang Z Y, Hong W and Suo Z 2005 *J. Mech. Phys. Solids* **53** 2101
[30] Zhou Y L, Niinomi M and Akahori T 2004 *Mater. Sci. Eng.* **371** 283
[31] Chaudhury M K, Finlay J A, Chung J Y, Callow M E and Callow J A 2005 *Model. Network. Biofouling* **21** 41
[32] Chan K S, Ji H, Wang X, Hudak S J and Lanning B R 2006 *Mater. Sci. Eng. A* **298**
[33] Chen Y F, Mei Y, Kaltofen R, Mönch J I, Schumann, Freudenberger J, Klauß H J and Schmidt O G 2008 *Adv. Mater.* **20** 3224
[34] Melzer M, Karnaushenko D, Lin G, Baunack S, Makarov D, Schmidt O G 2015 *Adv. Mater.* **27** 1333
[35] Li H H, Zhan Q F, Liu Y W, Liu L P, Yang H L, Zuo Z H, Shang T, Wang B M and Li R W 2016 *ACS Nano* **10** 4403